IEEE Access
Multidisciplinary | Rapid Review | Open Access Journal

Received November 5, 2019, accepted December 11, 2019, date of publication December 16, 2019,
date of current version December 26, 2019.

Digital Object Identifier 10.1109/ACCESS.2019.2959824

Beam Coverage Comparison of LEO Satellite Systems Based on User Diversification

SHIYI XIA[1], (Student Member, IEEE), QUANJIANG JIANG[1], CHENG ZOU[2], AND GUOTONG LI[1]

[1]Innovation Academy for Microsatellites of CAS, Shanghai 201203, China
[2]School of Information Science and Technology, ShanghaiTech University, Shanghai 201210, China

Corresponding author: Guotong Li (ligt@microsate.com)

ABSTRACT To achieve global network coverage and the need for high-speed communication, the idea of providing Internet access from space has made a strong comeback in recent years. The low earth orbit (LEO) communication satellite constellation is once again on the stage of the world with its unique features and new technology. In order to provide faster and more affordable communication resources, low-orbit satellites need be customized to design satellites. The beam coverage design is essential to the user-customized design. This paper combines the user traffic demand model and the low-orbit satellite beam coverage model to analyze the impact of beam coverage characteristics on the performance of low-orbit satellite systems. The user traffic model bases on the user simulative distribution (uniform, normal) and the user geographic distribution (according to the AIS and ADS-B historical data acquired by STU-2B and STU-2C which are the LEO satellites launched in Sep, 2015, Jiuquan, China). The beam coverage model compares the OneWeb system to the SpaceX system. The beam coverage model takes the variability in performance induced by atmospheric conditions for the user links into account. Follow that this paper proposes a system method to simulate the two satellite system which described by the throughput, delay, access probability. Finally, the sensitivity of beam coverage to user diversification is summarized and discussed.

INDEX TERMS LEO, communication satellite, comparison, beam, throughput, user distribution.

I. INTRODUCTION

A. MOTIVATION

According to the GSMA The State of Mobile Internet Connectivity 2019 report, there are 40% of the Earth's regions without network coverage. Due to differences in coverage areas, there are still 4 billion people on the planet who are unable to access the Internet [1]. In order to achieve seamless coverage of the global network, satellite Internet is essential. Therefore, satellite communications are attractive to both developed and developing countries because of their comprehensive coverage and large capacity. Low-Earth orbit (LEO) satellite networks is capable of achieving ubiquitous wireless coverage, and facilitating access to information in areas where terrestrial networks are difficult to deploy or cost-prohibitive. Besides, LEO satellites have a significant advantage over GEO satellites in terms of end-to-end delay and channel attenuation. A study shows that LEO satellites can meet more stringent delay requirements for voice and video transmission [2].

However, the low cost, small size, and lightweight of low-orbit satellites make the on-board power resources of low-orbit satellites severely limited. Due to the low orbital altitude and the speed of satellite motion, the coverage area of low-orbit satellites is continuously changing. In addition, according to the documentation requirements of ITU and national radio regulatory agencies, the priority of high-orbit satellite communications in most frequency bands is higher than that of low-orbit satellite communications, resulting in low-orbit satellites requiring switching frequencies when passing through some select regions or change the antenna angle to avoid interference with high-orbit satellite communications.

Further more, the distribution of user terminals in different countries and regions is different, and the service demand of different user terminals varies greatly. Low-orbit satellites

The associate editor coordinating the review of this manuscript and approving it for publication was Qiang Yang.

will face frequent switching frequency, dynamically changing user terminal distribution and sudden service requirements.

The point is that a successful low-orbit satellite commercial communication system should have the ability to flexibly adjust resource allocation based on the demand of terrestrial users.

That means the flexible use of on-board resources to provide faster and cheaper communication resources is a vital part of the LEO communication satellite design.

In the satellite design of the existing large-scale low-orbit satellite network companies, different low-orbit beam coverage designs have been adopted to meet the user diversification. OneWeb has launched 16 strips for coverage in order to provide global Internet access [3]. SpaceX will use phased array antennas to provide a large number of spot beams for flexible coverage [4]. TeleSat claims to be suitable for advanced digital communication payloads carrying DRA(Direct Radio Array). The DRA will be able to form at least 16 beams in the uplink direction and at least 16 additional beams in the downlink direction and will have the capability of beamforming, its power, bandwidth, size, number and boresight dynamically assigned to each beam to maximize system performance and minimize interference with GSO and NGSO satellites [5]. O3b aims to solve the problem of point-to-point communication, so the antenna is used: each satellite is equipped with 12 pairs of controllable butterfly antennas, 10 are user beams, each antenna can rotate ± 26 degrees to track the fixed position of the ground [6]. LeoSat intends to launch 78 satellites with 12 different widths of operable spot beams [7].

Considering the advantages and disadvantages of comparing multiple antenna coverage designs based on user service requirements and providing guidance for future satellite beam coverage designs, two typical beam coverages are selected. Flexible variable spot beam and highly elliptical beam with a large coverage. The representative of the flexible variable spot beam coverage is the Starlink satellite of the SpaceX low-orbit satellite constellation, and the representative of the fixed elliptical beam coverage is the satellite in the OneWeb low-orbit satellite constellation.

B. RELATED WORK

From a single system approach, a number of technical reports have been published (mostly proposed by the constellation designers themselves). Sturza [8] describes the original Teledesic satellite system.Patterson [9] analyzed 288 satellite systems resulting from the reduction of the original initial. Leopold comprehensively described the system in several papers [10], [11]. Wademan [12] analyzed the constellation of the global star(the technical aspect of the 924 satellites constellation).

Detailed system parameters are given in the above single system report, but a better system beam design cannot be obtained without comparison with other systems.

From the comparative approach, Evans [14] reviewed the Globalstar, Iridium, and Odysey systems by comparing methods, focusing on each proposed system architecture, handset design and cost structure. GEO, MEO and LEO), later compared different recommendations for the Ka-band system in LEO [15]. Shaw [16] quantitatively compared the functions of cyber star, Spaceway and Celesti, which evaluated the capacity, signal reduction.Inigo [17] compared some of the indicators of OneWeb, SpaceX, TeleSat three low-orbit satellite networks, using a a new statistical framework to estimate the explosion of the entire system.

In the comparison approach, there is a lack of system analysis on user diversification adaptability. Population number is used in [17] to analyze the difference of ground users which has some guidance. However, there is a further lack of adaptability analysis for the satellite user group (such as high altitude, ocean).

C. CONTRIBUTION

This paper reviews the beam characteristics and link budgets described in the respective FCC documents (and later press releases) of these two low-orbit satellite systems. In order to demonstrate the validity and rationality of two different beam coverage designs:

- 1. The low-orbit satellite user demand model is analyzed and divided into two parts, one is the user simulative model (uniform, gaussian) and the other is the user demand model (aircraft, ship) of a certain area to give and establish the user traffic model.
- 2. Calculate the authentic link budget and beam characteristics based on the FCC data of SpaceX and OneWeb. Establish two different satellite beam coverage models based on the ITU atmospheric attenuation model.
- 3. According to the satellite user distribution, traffic, and resource demand model, the simulation is combined with two satellite coverage models.
- 4. According to the simulation results, the effective throughput performance, transmission success performance, and delay performance of each satellite under different simulated and practical scenarios are obtained.
- 5. Combine the previous review and comparison of simulation results, discuss and draw conclusions.

D. PAPER STRUCTURE

In chapter II, a brief review of OneWeb and SpaceX satellites is carried out. The Chapter III builds a simulation model, in which the user traffic model and the low-orbit satellite beam coverage model are established respectively, and the system performance parameter calculation method is proposed. Chapter IV analyze the simulation results and discuss the beam coverage methods of OneWeb and SpaceX; Chapter V is the conclusion.

II. THE LEO SATELLITE SYSTEM

A. THE ONEWEB SYSTEM

On June 22, 2017, the Federal Communications Commission (FCC) approved OneWeb's request to deploy a global

network of 720 LEO satellites using Ka (20/30 GHz) and Ku (11/14 GHz) bands to provide global Internet connectivity. Oneweb plans to launch its first ten satellites in early 2018. Fierce Wireless reports that OneWeb will use its rocket to accomplish its mission. After testing, broadband services will be fully launched in Alaska after 2019, and then continue to expand to more regions in 2020, eventually serving the world.

OneWeb satellite payload is in the form of transparent forwarding respectively. Each satellite has 16 identical user beams, each of which has a fixed highly elliptical point beam, working in the Ku band. The upstream user link frequency is 12.75-13.25 GHz, 14.0 GHz-14.5 GHz, and the downlink user link frequency is 10.7-12.7 GHz. In addition, each satellite has two uniformly operable aperture antennas in the Ka-band. Each antenna can produce an independently operable circular point beam. Each satellite service area 1080 km*1080 km, the capacity is 7.5 Gbps, the entire constellation is 6-7 Tbps. The downlink rate of a single beam can reach 750 Mbps, and the upstream rate is 375 Mbps. Download: 16 Ku downlink channels, each channel corresponds to a Ku band solid-state power amplifier, a total of 16 SSPAs. Uplink Load: Four Ka solid-state power amplifiers, one feed beam for each amplifier and eight channels for each amplifier.

B. THE SPACEX SYSTEM

The system aims to provide a wide range of broadband and communication services for residential, commercial, institutional, government, and professional users worldwide. Advanced phased-array beamforming and digital processing technologies in satellite payloads enable the system to use Ku and Ka-band spectrum resources efficiently and share the spectrum flexibly with other licensed users. User terminals using SpaceX systems will use similar phased array technology to allow altitude indication and directed antenna beams of low Earth orbit satellites in tracking systems. The system will use optical inter-satellite links for seamless network management and service continuity, which will also facilitate compliance with radiation restrictions aimed at promoting spectrum sharing with other systems.

SpaceX's Ku + Ka constellation contains 4,425 satellites distributed over several sets of orbits. The first core constellation to be deployed consists of 1600 satellites, which are evenly distributed on 11 orbital planes with an orbital altitude of 1150 km and an inclination of 53. The other 2,825 satellites will be deployed in minor deployments.

Each satellite in the SpaceX system will carry a high-level digital payload containing phased array antennas, which will allow each beam to turn and form independently. The minimum elevation of the user terminal is 40, and the total throughput of each satellite is estimated to be 17-23 Gbps, depending on the characteristics of the user terminal.

SpaceX system will use the Ku-band for user communication, and gateway communication will be carried out in Ka-band. In particular, 10.7 - 12.7 GHz and 14.0 - 14.5 GHz bands will be used for downlink and uplink

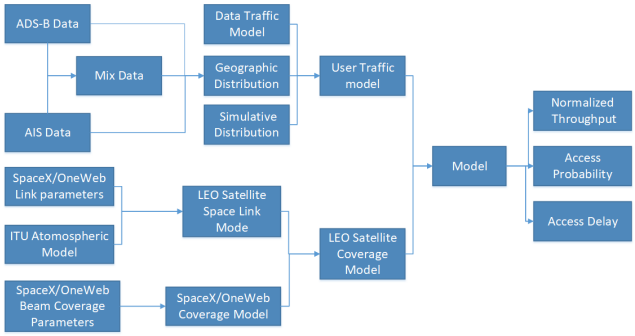

FIGURE 1. Overall of system model.

user communications respectively, while downlink and upstream gateway communications will use 17.8 - 19.3 GHz and 27.5 - 30.0 GHz bands respectively.

The satellite user beam is independently controllable, and the elevation of the user terminal is at least 40 degrees. Phased array antenna beam expands, and the increase of the ground point beam area leads to the increase of the distance from the satellite to the ground, which is aggravated by the curvature of the earth,thus increasing interference.

SpaceX solves this problem by closing the phased array antenna element at a certain angle. Satellite Signal Gate Station Beam: Each satellite sends two Ka beams (RHCP and LHCP) with the same frequency. Each Ka beam can only communicate with one Signal Gate Station at one time.

Satellite Ka-beam GT values are 11.4-13.7 dB/K. EIRP maximum: - 11.07 dBW/4KHz, - 14.2 dBW/4KHz.

Satellite Ku-beam GT values are 8.7-9.8 dB/K. EIRP maximum value: 18.64 dBW/MHz, minimum about 15.6 dBW/MHz.

User beams and station beams are spot beams with angles of 1.5 and 1 respectively. These beams are divided into the bandwidth of 7.8125 MHz and a total width of 1 GHz.

The system uses phased array technology to dynamically control a large number of beams and centralize the capacity on demand.

III. METHOD AND MODEL DESCRIPTION

A. MODELING OF SATELLITE COVERED CELLS

The low-orbit satellite coverage area can be divided into a plurality of neatly arranged big circle blocks, and each circular block is defined as one cell ($cell_i$). Let the time length T of each $cell_i$ covered by the satellite, and the number of users in each $cell_i$ is $number_i$. Combine the beam coverage features of SpaceX and OneWeb in Table 1, for each circle $cell_i$ is further divided into a plurality of K equal-sized spot beam regions or H equal-sized oval beam regions, and each beam coverage region is defined as one *unit*, which is recorded as shown in Fig.2, the large circle on the outside represents a cell in blue, the small circle in red represents SpaceX's spot beam coverage, and the black oval represents OneWeb's elliptical beam coverage.

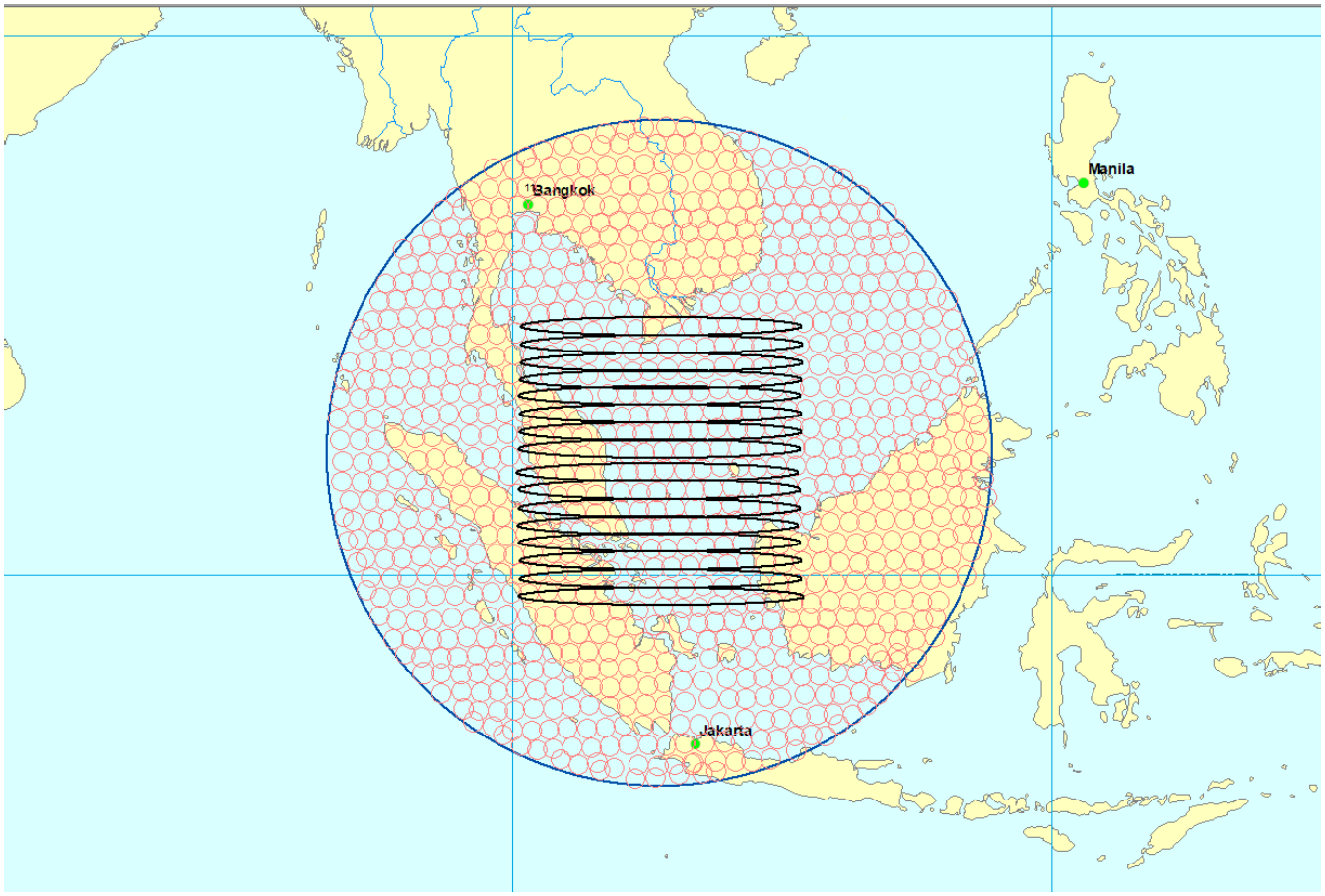

FIGURE 2. SpaceX and OneWeb satellite cover in Malaysia.

TABLE 1. Beam characteristics.

Symbol	SpaceX	OneWeb	
$Numberofbeams$	≥ 8	16	
$Controllability$	Yes	No	
$Beamforming$	Yes	No	
$Coveragearea$	2800	75000	km^2
$BandWidth$	250	250	MHz

B. ATMOSPHERIC MODELS

In satellite communication links, the communication link is susceptible to atmospheric attenuation due to the long transmission distance. At the KA-band frequency, atmospheric attenuation can cause link capacity to drop, sometimes even wholly interrupting in a non-negligible time. In order to deal with time-varying fading and maximizing the amount of link data, adaptive techniques are usually adopted after forwarding channel estimation, and protocol support using adaptive modulation coding is already included in DVB-S2X.

In this paper, we apply the ITU recommended atmospheric attenuation model following the guidelines provided in recommendation ITU-R P.618-13 [18], (which considers gaseous, clouds, tropospheric Scintillation, and rain impairments). These models provide a relationship between the attenuation contribution values due to each of the above events and the percentage of time that exceeds these values (i.e., the cumulative distribution function (CDF) of atmospheric attenuation contributions).In this paper, gas attenuation and cloud attenuation are calculated using the recommended models in ITU-R P.676-11 and ITU-R P.840-7, respectively, while the maps in recommendations ITU-RP.837-6, ITU-RP.838-3 and ITU-R P.839-4 reused to estimate the rainfall-rate, rain specific attenuation, and rain height respectively.

C. LINK BUDGET MODEL

The link budget module is combined with the atmospheric model to calculate the reachable data rate for uplink and downlink communications under different atmospheric conditions.

For our performance estimation model, we assumed that the modulation-coding schemes prescribed in the standard DVB-S2X [22], developed by the Digital Video Broadcast Project in 2014, are used, since it is the predominant standard for broadcasting, broadband satellite communication, and interactive services. The standard defines the framing

TABLE 2. Low-orbit satellite link budget of SpaceX & OneWeb.

Symbol	SpaceX	OneWeb	
$Frequency$	13.5	13.5	GHz
$Bandwidth$	0.25	0.25	GHz
$EIRP$	36.71	34.6	Dbw
$MODCOD$	16APSK 2/3	16APSK 3/4	
$Roll-off$	0.1	0.1	
$Spectrum\ efficiency$	2.4	2.7	Bps/Hz
$Path\ distance$	1504	1684	Km
$Elevation\ angle$	50	40	deg
$Space\ loss$	178.6	179.6	dB
$Atmospheric\ loss$	0.41	0.53	dB
$RX\ antenna\ size$	0.75	0.7	m
$RX\ antenna\ gain$	38.3	37.7	dBi
$System\ temperature$	350.1	362.9	K
$RX\ C/N0$	10.5	12	dB
$RX\ C/ASI$	25	25	dB
$RX\ C/XPI$	20	22	dB
$HPA\ C/3IM$	30	25	dB
$RXEb/(N0+I0)Width$	5.9	6.7	MHz
$Eb/N0\ threshold$	5.2	5.9	dB
$Linkmargin$	0.76	0.82	dB
$Datarate$	599.4	674.3	Mbps
$Shannonlimit$	1.49	1.46	dB

structure, channel coding, and a set of modulation schemes. In particular, more than 60 MODCODs are included, with modulations ranging from BPSK to 256-APSK and coding rates from 1/4 to 9/10.

In addition, we assume that the output backoff of the solid state power amplifier is equal to the peak average power ratio of the MODCOD (given the ratio of the percentile power to the average power of 99.9%) to avoid distortion caused by saturation.

In Table.2 we obtained the remaining parameters from the detailed FCC file submitted by SpcaeX and OneWeb, including the antenna diameter of the transmitter and receiver, the efficiency and noise temperature, the different loss values on the RF link and the carrier interference.

D. USER TRAFFIC MODEL

In order to get the effective performance of the system, we have established a user distribution and demand model, which is divided into a model that simulates the user distribution and the geographic position distribution of the user.

Let user $user_{ij}(t)$, $(x_{user_{ij}}, y_{user_{ij}}, d_{user_{ij}}(t))$, the user's position coordinate $x_{user_{ij}}, y_{user_{ij}}$.In the low-orbit satellite system, because the satellite moves faster, the motion of the ground user can be ignored in the relative motion with the satellite. As a consequence this

article simplifies the user distribution model, assuming that the user's geographic location is static and user $user_{ij}(x_{user_{ij}}, y_{user_{ij}})$ is randomly distributed in the service coverage area $cell_i$. $D_{user_{ij}}(t)$ is a user request for data volume within the satellite coverage time $(t, t+\delta t)$, $\delta t$is the maximum delay time.

Firstly the user distribution modeling of low-orbit satellites is modeled separately using simulated mathematical models

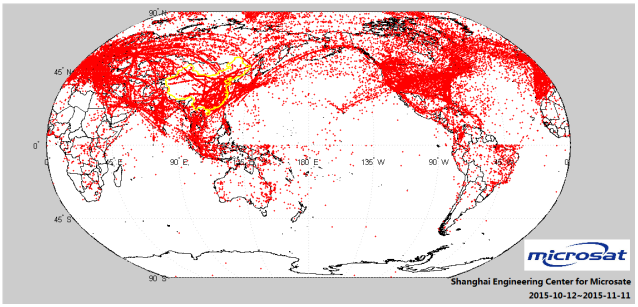

FIGURE 3. STU-2C ADS-B received data from October 12 to November 11, 2015.

and models abstracted from factual scenes. The simulated model uses two random distributions, uniform distribution, and a normal distribution.

Therefore the two-dimensional random variables $(X_{user_{ij}}, Y_{user_{ij}})$can obey the uniform distribution, the two-dimensional normal distribution, and the practical user distribution.

Because the user terminal antenna of the low-orbit broadband satellite needs a high cost, the part of the terrestrial service should avoid competing with the 5G network as a supplement to the 5G network. For complementing the 5G network, its application should be outside the application area covered by the current 5G network. Low-orbit satellite communications should complement the 5G network application areas, and should focus on areas with high technology relevance, which can be expressed as follows:

- Land network coverage blind areas (special communication needs such as deserts, mountains, and remote villages);
- Disaster areas (emergency communications such as earthquakes, tsunamis, tornadoes, wars, etc.);
- High altitude (aircraft, hot air balloon, high altitude drone, etc.);
- Ocean (offshore vessels, deep-sea oil and gas platforms, marine meteorological sensor networks, etc.);
- Polar (South, North Pole).

In summary, we choose aircraft AIS data and ship ADS-B data for high-altitude and marine user distribution. The ADS-B data collects global air traffic information through the onboard ADS-B receiver carried by the satellite STU-2C. The AIS data collects global maritime traffic information through the onboard AIS receiver carried by the STU-2B. As shown in the figure, the data accumulation graph for the STU-2C for one month (October 12-November 11, 2015).

1) UNIFORM USER DISTRIBUTION

If the two-dimensional random variable $(X_{user_{ij}}, Y_{user_{ij}})$ has a probability density function

$$f(x_{user_{ij}}, y_{user_{ij}}) = \begin{cases} 1/A, & (x_{user_{ij}}, y_{user_{ij}}) \in cell_i \\ 0, & otherwise \end{cases} \quad (1)$$

Then the user obeys a uniform distribution on $(X_{user_{ij}}, Y_{user_{ij}})$.

2) NORMAL DISTRIBUTION

Let the user's $user_{ij}(x_{user_{ij}}, x_{user_{ij}})$ have the abscissa $x_{user_{ij}}$ and the ordinate $y_{user_{ij}}$independent of each other, if the two-dimensional random variable $(X_{user_{ij}}, Y_{user_{ij}})$has Probability density function

$$f(x_{user_{ij}}, y_{user_{ij}}) = \frac{1}{2\pi\sigma_1\sigma_2} \exp\{-\frac{1}{2}[\frac{(x_{user_{ij}}-\mu_1)^2}{\sigma_1^2} + \frac{(y_{user_{ij}}-\mu_2)^2}{\sigma_2^2}]\} \tag{2}$$

Then the user $(X_{user_{ij}}, Y_{user_{ij}})$ obeys the two-dimensional normal distribution with parameters $\mu_1, \mu_2, \sigma_1^2, \sigma_2^2, \rho = 0$, recorded as

$$(X_{user_{ij}}, Y_{user_{ij}})\tilde{\mathrm{N}}(\mu_1, \mu_2, \sigma_1^2, \sigma_2^2, \rho = 0) \tag{3}$$

The probability that user $user_{ij}(x_{user_{ij}}, y_{user_{ij}})$ falls into $cell_i$ is

$$\begin{aligned} &P\{(x_{user_{ij}}, y_{user_{ij}}) \in cell_i\} \\ &= dx_{user_{ij}} dy_{user_{ij}} \\ &= \int_{x_1}^{x_2}\int_{y_1}^{y_2} \frac{1}{2\pi\sigma_1\sigma_2} \exp\{-\frac{1}{2}[\frac{(x_{user_{ij}}-\mu_1)^2}{\sigma_1^2} + \frac{(y_{user_{ij}}-\mu_2)^2}{\sigma_2^2}]\} \\ &\quad dx_{user_{ij}} dy_{user_{ij}} \end{aligned} \tag{4}$$

3) GLOBAL GEOGRAPHIC USER DISTRIBUTION ANALYSIS

According to the ADS-B and AIS data received by STU-2B,STU-2C, the airplane position information of one month can be easily seen. The distribution of aircraft and ships is not uniform on a global scale, as shown in Fig. 4, Fig. 5. More detailed analysis, ships mainly concentrated in the vicinity of ports and ship routes. Due to the restrictions of the mainland and ocean currents and reefs, the routes of ocean-going vessels are fixed, thus the distribution of ships is closer to a fixed non-uniform distribution. As shown in the Fig. 4, the aircraft does not have restrictions on the continental plate and the ocean. The distribution constraints of the aircraft are only that the routes between the aircraft do not interfere with each other. In addition to this, the aircraft is concentrated in the vicinity of developed cities. The aircraft is more dispersed than the ship. As shown in Fig. 6 when the aircraft and ship scenes are compositely distributed, we get a composite user scene distribution.

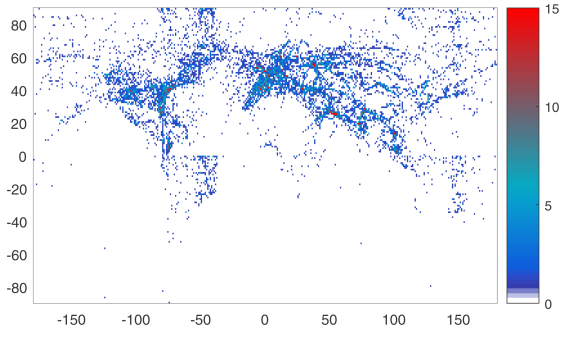

FIGURE 4. World plane user distribution.

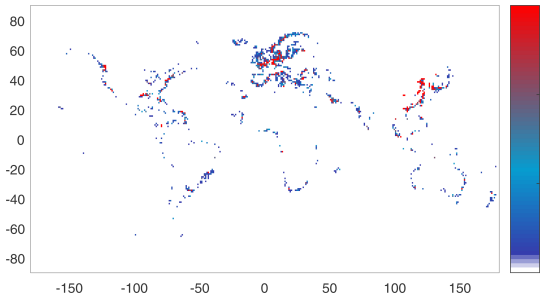

FIGURE 5. World ship user distribution.

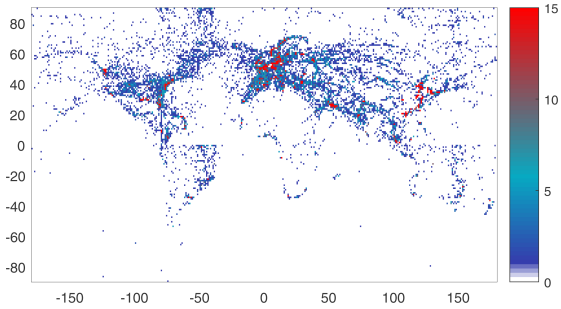

FIGURE 6. World hybird user distribution.

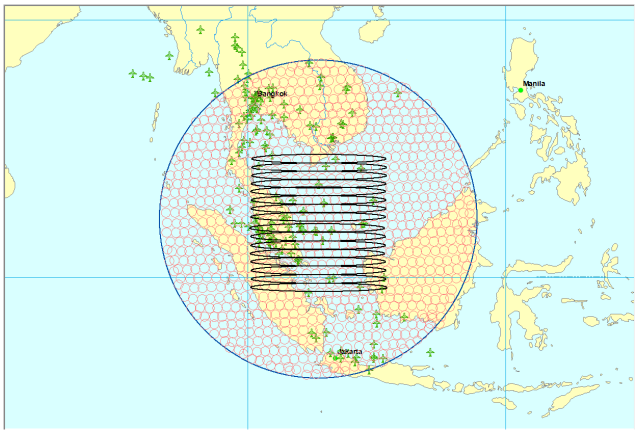

FIGURE 7. Real-time plane user distribution in Malaysia.

4) REAL-TIME UNDER-THE-USER DISTRIBUTION

Then we set up the authentic satellite coverage scene distribution characteristic model. According to the ADS-B and AIS received by STU-2B and STU-2C, tthe position information of the aircraft and the ship that are not repeated in the T coverage at the same time is selected.The user geographic distribution location information $user_{ij}(x_{user_{ij}}, y_{user_{ij}})$ is set as the location information of each user $user_{ij}(x_{user_{ij}}, y_{user_{ij}})$.

E. DEMAND MODEL

At a certain moment t, if the average traffic strength set of all $user_{ij}$ in the target area $cell_i$ is $Traf_{ij}(t)$(bps), the

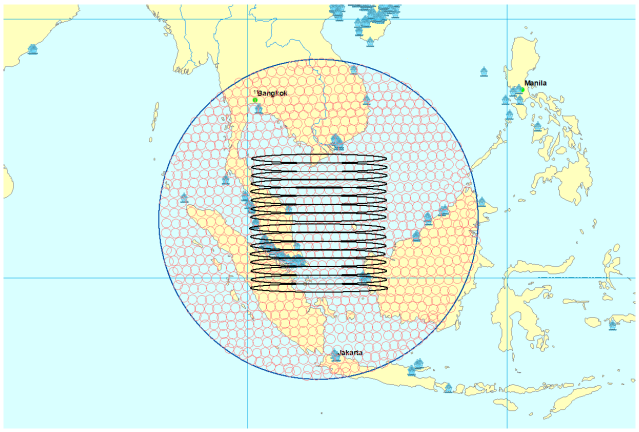

FIGURE 8. Real-time ship user distribution in Malaysia.

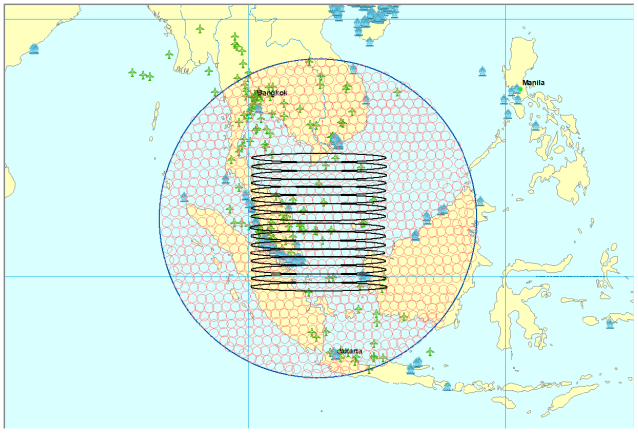

FIGURE 9. Real-time hybrid user distribution in Malaysia.

traffic of the user in $cell_i$ can be modeled as a set $R = \{(x_{user_{ij}}, y_{user_{ij}}, Traf_{iuser_{ij}}), user_{ij} \leq number_i\}$.

The "user" here is a ground hotspot terminal, and the quality factor G/T value of each user is different. Let L_p be the link power loss and EIRP be the equivalent isotropic radiation power. Therefore, the link carrier-to-noise ratio C/T can be expressed in the form of dB:

$$C/T = EIRP - L_p + G/T \tag{5}$$

Among them, the G/T value and the C/T value are user-specific parameters, and L_p is known. Therefore, the parameter that can be used to characterize the difference of the user $user_{ij}$ is only the $EIRP$ value, which is expressed as $EIRP_{user_{ij}}$;

Extraordinary, the bandwidth requirement of the user $user_{ij}$ is $B_{user_{ij}}(t)$ is uniformly distributed within $(0, T)$, and the service request uses Poisson distribution to generate a service request within $(0, T)$, and the minimum slot resolution is $\tau = 1ms$, a user generates only one bandwidth requirement in $(t, t + \tau)$. Thus, the attribute vector of the user $user_{ij}$ is $(EIRP_{user_{ij}}, B_{user_{ij}}t)$, and the relationship between the attribute and the average traffic intensity of the user is $Traf_{ij}(t)$, which can be expressed as:

$$Traf_{ij} = f(EIRP_{user_{ij}}, B_{user_{ij}}(t)) \tag{6}$$

Therefore, at time t, the traffic of the user in $cell_i$ can be equivalently modeled as the average resource service demand of the user, expressed as

$$R \Leftrightarrow \{(x_{user_{ij}}, y_{user_{ij}}, EIRP_{user_{ij}}, B_{user_{ij}}(t)), user_{ij} \leq number_i\} \tag{7}$$

Conclusively, the non-uniform traffic model in the target area $cell_i$ is modeled as a resource requirement set of the user.

F. SYSTEM PERFORMANCE METRICS

1) NORMALIZED SYSTEM THROUGHPUT

In order to facilitate statistics and simplify the calculation, a normalized system throughput concept is proposed to measure the system beam resource utilization efficiency of the SpaceX beam coverage and the OneWeb beam coverage. Normalized system throughput is a concentrated expression of system throughput performance, such as the value range, when the normalized system throughput is 1, that is, the system throughput is equal to the total throughput that can be provided by the on-board beam, indicating the current on-board beam resources are maximized.

$$Normalized\ system\ throughput = \frac{User\ traffic}{Total\ satellite\ throughput} \tag{8}$$

2) SUCCESSFUL TRANSMISSION PERFORMANCE

The transmission success performance statistic is the packet statistic that completes the packet processing within the maximum delay within the period T.

$$P_{success} = \frac{N_{success}}{N_{all}} * 100\% \tag{9}$$

This value indicates how much the satellite can complete the queuing service during the change in user traffic demand.

3) TIME DELAY PERFORMANCE

In addition to system beam resource utilization efficiency, another important parameter to consider is the analysis of system delay, the overall delay of the packet. In any data communication network, data packets will have system delay due to propagation delay, queuing and buffering, and low-orbit satellite hop beam communication systems are no exception. The total end-to-end delay of satellite communication consists of communication transmission delay, data processing delay and queuing delay [19], where the communication transmission delay depends on the distance between the satellites links, low-orbit satellites and high-orbit satellites. Due to the difference in transmission distance, the transmission delay of satellite communication is completely different from that in terrestrial communication. The data processing delay depends on the processing speed of the on-board payload data and is generally approximated as a constant. The queuing

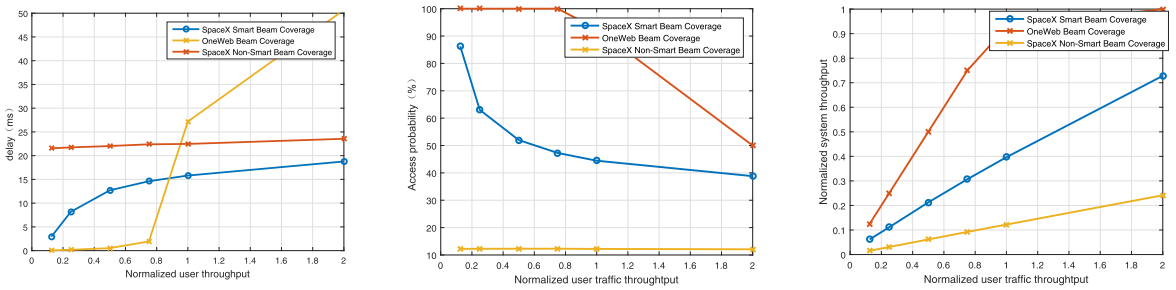

(a) Access delay (b) Access probability (c) Normalized system throughput

FIGURE 10. **Uniform user distribution system performance.**

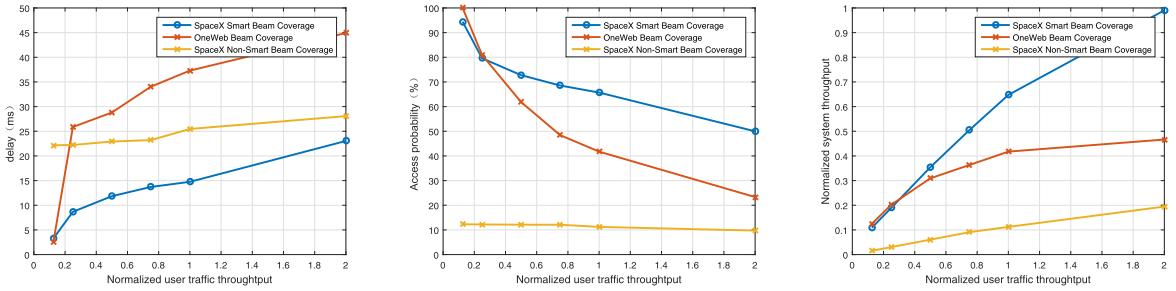

(a) Access delay (b) Access probability (c) Normalized system throughput

FIGURE 11. **Normal user distribution system performance.**

delay is the only controllable delay. If the on-board buffer is large enough, the queuing delay will be considerable. The total time when the packet arrives at the gateway can be expressed as

$$\tau_{delay} = \tau_{pgs} + \tau_{process} + \tau_{que} + \tau_{pld} = \tau_{que} + \tau_{ser} \quad (10)$$

where τ_{delay} is the total delay, $\tau_{pgs}$is the communication transmission delay, $\tau_{process}$ is the data processing delay, τ_{que} is the queuing delay, and τ_{pld} is the load inherent delay.

In the simulation analysis of this paper, the queuing delay is equated with the system delay performance. Delay derivation of the packet p of beam i. The dwell time of the packet is recorded as w_i^{soj}, and its value is equal to the difference between the time $t_i^f(p)$ at which the packet leaves and the arrival time $t_i^a(p)$ of the packet. The average queuing delay refers to the statistical average of the dwell time of the packet, also known as the average packet dwell time, which can be obtained by statistical summation of the average packet queuing time and the average packet service time, as follows:

$$\begin{aligned} E[w_i^{soj}] &= \lim_{K\to\infty} \frac{1}{K} \sum_{p=1}^{K} [t_i^f(p) - t_i^a(p)] \\ &= E[w_i^{que}] + E[w_i^{ser}] \leq \Delta \end{aligned} \quad (11)$$

where K is the maximum number of packets that can be served by each beam, $E[w_i^{soj}]$ is the average queuing delay in the statistical beam i, $E[w_i^{que}]$ is the average packet queuing time in the statistical beam i, and $E[w_i^{ser}]$ is the average packet service time in the statistical beam i., Δ is the maximum critical value of the average queuing delay (beyond the threshold, the packet is retransmitted, in this paper $\Delta = 50ms$).

IV. RESULT

The simulation is performed by the beam coverage, user, and traffic model established in the previous section. On account of whether the SpaceX constellation has an antenna that is available to sense user traffic, we divide the SpaceX beam coverage into smart and non-smart beam coverage for simulation. OneWeb uses the OneWeb overlay model created in Chapter II. The system throughput, access probability, and access delay in this paper refer to the performance of the access layer, rather than the end-to-end transmission performance. The access delay calculation does not consider user data that failed to transmit. Therefore, the analysis of transmission delay have to combined with the access probability.

A. USER SIMULATIVE DISTRIBUTION

As shown in Fig 10-11, the relationship between user traffic requirements of user simulative distribution and the three system metrics is evidently. As the user traffic demand increases, whatever the user distribution is, the delay and the system throughput performance are on the rise, and the access success probability is declining.

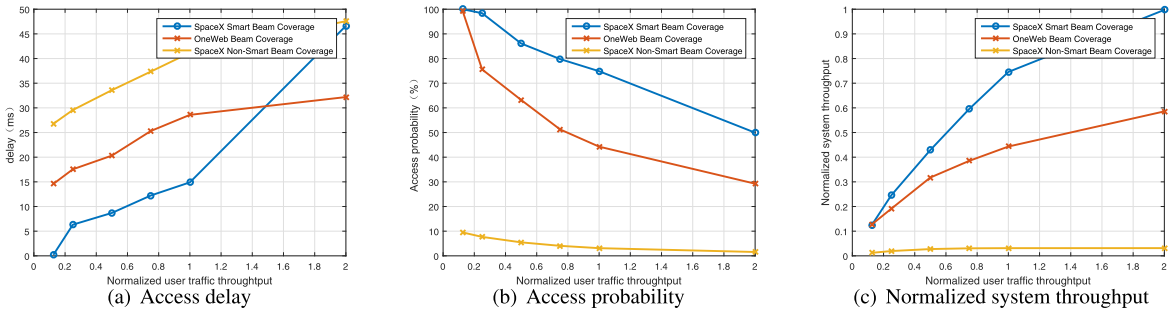

(a) Access delay (b) Access probability (c) Normalized system throughput

FIGURE 12. Ship user distribution system performance.

Fig.10 shows the performance of the uniform user distribution system. In Fig.10(c), when the normalized user traffic is less than the total onboard performance, OneWeb's access delay is less than 30*ms*, and the access probability is almost 100%.And when the user demand is almost 1, OneWeb's fixed beam coverage can fully maximize system performance and maximize system utilization. In contrast, SpaceX's smart beam coverage has not increased by more than 20ms in Fig.10(c) as the user's demand increases. However, the access probability as shown in Fig.10(b) that decreases rapidly and is significantly smaller than the OneWeb beam coverage. Not only that as shown in Fig.10(a) that the SpaceX system's throughput performance is not fully utilized. Non-smart antennas have access delay, but the access probability and system throughput are very low.

The reason is mainly that the user distribution is relatively uniform, the user distribution range is large, and the SpaceX beam spot coverage area is small. Consequently, it is needed to repeatedly switch the spot beams, and the system wastes too much on repeated switching and establishing connection.

Fig.11 shown that the system performance of the user location which obey normal distribution. As is reflected in Fig.11(a), the access delay of SpaceX is the smallest when the normalized user traffic before 1.6.Combined with the Fig.11(b) analysis, the access probablity of SpaceX also decreases with the user traffic increase. But the rate of decline is slower than OneWeb. In Fig.11(c), SpaceX's satellite normalized throughput performance is better than OneWeb's performance by 24% at the user traffic demand is equal to the maximum throughput that the satellite can provide.And SpaceX is better than OneWeb 53% in twice the maximum throughput that the satellite can provide.

The resources on the satellite, while OneWeb can not quickly use the on-board resources when it is evenly distributed. With the increase in business volume, the performance of SpaceX is also increasing rapidly. When the users are unevenly distributed, the flexibility of SpaceX satellite smart beam coverage can be more reflected.

SpaceX is able to allocate resources according to user needs, which is more flexible than OneWeb. For users with normal distribution, the OneWeb beam coverage is limited by the fixed beam resources, and cannot meet the differentiated requirements of different user distributions. Therefore, the system throughput performance is significantly reduced compared with the uniform distribution, while the SpaceX solution advantage is uneven in the user. The distribution is further reflected, which is that SpaceX can better adapt to user needs and be more flexible in resource allocation.

B. USER GEOGRAPHIC DISTRIBUTION

According to the simulation analysis of the simulated distribution, we know that the advantages and disadvantages of the SpaceX smart beam converage and the OneWeb fixed beam coverage under different user distributions are difficult to demonstrate.

Following that, this paper replacing the user distribution with the latitude and longitude position data of the aircraft and the ship to further analyze the impact of beam coverage on system performance.

As is shown in Fig.12 the system performance of the SpaceX smart beam coverage is better than the OneWeb fixed beam coverage.The reason is that ships are more geographically concentrated. The distribution is more complex and non-uniform user distribution.In Fig.13(b)(c), The access probability and system throughput performance of SpaceX smart beam coverage is almost equal to OneWeb. However, it is worth noting that the access delay performance of in Fig.13(a) SpaceX is better than Oneweb 15ms.The access probability and system throughput performance of SpaceX with non-smart beam coverage is still low.

In Fig.14(a)(b), in the hybrid scenario with ship and aircraft users, when the normalized user traffic demand is less than 0.3. The access delay of the SpaceX smart beam coverage is greater than the access delay of OneWeb. This is the price at which the beam needs to be switched. When the user normalized traffic is greater than 0.5, the advantages of SpaceX begin to become apparent. At the normalized user demand is 1, the normalized system throughput of in Fig.14(c) SpaceX is 10% better than the OneWeb system.

According to the hybrid user distribution scenario simulation, it can be concluded that SpaceX's smart beam coverage can cope with different user distribution scenarios and show better flexibility, while OneWeb's satellite flexibility is

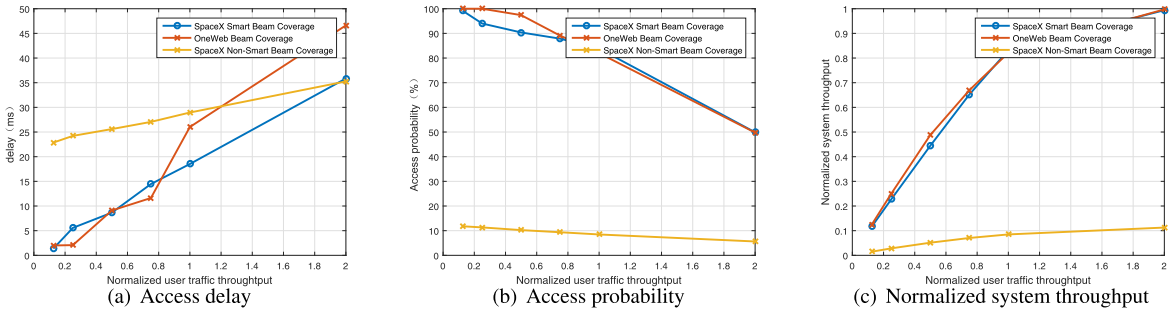

(a) Access delay (b) Access probability (c) Normalized system throughput

FIGURE 13. Plane user distribution system performance.

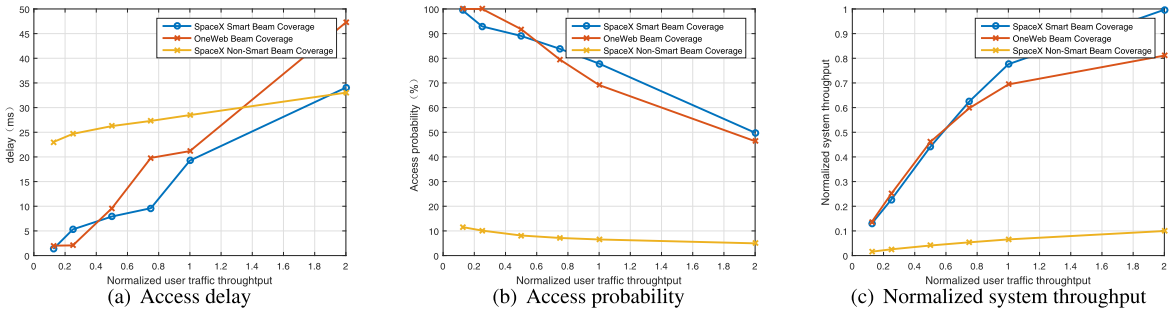

(a) Access delay (b) Access probability (c) Normalized system throughput

FIGURE 14. Hybrid user distribution system performance.

TABLE 3. Numerical result of system performance.

Normalized User Traffic		1	2	1	2	1	2
User Distribution	LEO System	Average Access Delay(ms)		Access Probability(%)		Normalized System Throughput	
Uniform	OneWeb	27.191	50.684	92.626	49.992	0.92625	0.99984
	S-SpaceX	15.812	18.777	44.449	38.808	0.39658	0.72817
	NonS-SpaceX	22.47	23.557	12.206	12.076	0.122206	0.24151
Normal	OneWeb	37.2992	44.9292	41.7474	23.3227	0.4175	0.4664
	S-SpaceX	14.749	23.0343	65.5955	49.9844	0.6474	0.9904
	NonS-SpaceX	25.4636	28.0682	11.2198	9.7278	0.1122	0.1946
Ship	OneWeb	28.5798	32.1903	44.2693	29.2549	0.4432	0.5857
	SpaceX	14.8991	46.6243	78.8624	49.9394	0.7456	0.9973
	NonS-SpaceX	41.1816	47.5667	3.1138	1.5608	0.0312	0.0313
Plane	OneWeb	26.0207	46.6201	81.9745	49.7667	0.8214	0.9973
	S-SpaceX	18.5188	35.85	83.85276	49.8927	0.8319	0.994
	NonS-SpaceX	28.954	35.2593	8.4649	5.6207	0.0848	0.1126
Hybrid	OneWeb	27.1796	47.2619	77.8727	49.9192	0.7849	0.8394
	S-SpaceX	19.2586	34.0538	81.5502	49.9424	0.8148	0.9947
	NonS-SpaceX	28.4833	33.0271	8.2502	5.9167	0.0832	0.1185

insufficient, but it is still weak when users are more dispersed ability.

C. DISCUSSION

As the simulation results shown in Table 3, we can clearly know that the two coverage modes have different performances when facing different user distributions, so the objects of the two low-orbit satellite network services should be different.

OneWeb should target users who are scattered on a latitude scale, such as aircraft users and users with evenly distributed ground. Because the throughput performance of the Oneweb system has reached 0.92625 in uniform user distribution.This data is better than SpaceX smart beam coverage which has reached 0.39658.Furthermore, the OneWeb system throughput 0.8214 is similar from SpaceX throughput 0.8319.

SpaceX's coverage design should be a universal beam coverage design, which has a better throughput performance delay(15.812 in uniform, 14.749 in normal, 14.8991 in ship, 18.5188 in plane, 19.2586 in hybird) and access probability(44.449 in uniform, 65.5955 in normal, 78.8624 in ship, 83.85276 in plane, 81.5502 in hybird) for most user distribution. In this paper, the SpaceX smart beam switching method uses a simple on-demand allocation algorithm, so SpaceX

performance can be further improved by improved algorithms. The resulting throughput loss or reduced beam jitter times, as well as positioning users to more concentrated users such as ship user services.

V. CONCLUSION

Low-orbit satellite communication networks should ensure communication anywhere, anytime, in an open environment. From the perspective of communication accessibility and real-time performance, compared with high-orbit communication satellites, low-orbit satellite has the advantages of polar coverage and low latency. Compared with terrestrial networks, its advantages are space-based and global flawless coverage. But it also has obvious power constraint defects. It means that using resources more flexible is indispensable in LEO satellite design.

This paper aims to verify the impact of beam coverage on the performance of LEO satellite systems. Explore ways to find better beam coverage by verifying existing systems. At present, the two satellite companies designed by the two satellite companies, SpaceX and OneWeb, use different beam coverage to achieve flexible resource allocation. This paper investigates authentic satellite link parameters, beam coverage characteristics, user distribution, establishes low-orbit satellite beam coverage model, user service, traffic model, and uses effective throughput, access delay, data transmission performance and other indicators for the two satellite systems.

According to the simulation results of the user's geographical distribution model, SpaceX spot beam coverage can better meet the needs of users, and it can outperform OneWeb16 fixed beam coverage in both aircraft and ships. Even on aircraft users, the performance of the two is almost the same, but the access delay on SpaceX is 15*ms* smaller than OneWeb. Therefore this paper obtains the excellent performance of SpaceX satellite in the user geographic service distribution process regardless of the user distribution. The OneWeb beam coverage design will have a large waste when the user is concentrated in latitude.

In the next decade, we believe that with the further expansion of the low-orbit satellite constellation scale, the mass production of satellites has become an inevitable trend. Designing satellites should create a uniform, highly compatible architecture, so beam coverage should be similar to SpaceX's flexible beam coverage, and even more flexible. User-specific algorithm development on a unified architecture will become a magic weapon for the performance of different low-orbit satellite systems. We will also focus on further research on unified, flexible architecture beam coverage in future work.

REFERENCES

[1] K. Bahia and S. Suardi, "The state of mobile Internet connectivity 2019," GSM Assoc., London, U.K., Tech. Rep. Jul. 2019. [Online]. Available: https://www.gsma.com/mobilefordevelopment/wp-content/uploads/2019/07/GSMA-State-of-Mobile-Internet-Connectivity-Report-2019.pdf
[2] Q. Yang, D. I. Laurenson, and J. A. Barria, "On the use of LEO satellite constellation for active network management in power distribution networks," *IEEE Trans. Smart Grid*, vol. 3, no. 3, pp. 1371–1381, Sep. 2012.
[3] WorldVu Satellites Limited. *OneWeb Ka-Band NGSO Constellation FCC Filing SAT-LOI- 20160428-00041*. Accessed: Dec. 9, 2018. [Online]. Available: http://licensing.fcc.gov/myibfs/forwardtopublictabaction.do?file number=SATLOI2016042800041
[4] Space Exploration Holdings. *LLC, SpaceX Ka-Band NGSO Constellation FCC Filing Sat-LOA-20161115-00118*. Accessed: Dec. 9, 2018. [Online]. Available: http://licensing.fcc.gov/myibfs/forwardtopublictabaction.do?file number=SATLOA2 016111500118
[5] Telesat Canada. *Telesat Ka-Band NGSO Constellation FCC Filing SAT-PDR-20161115-00108*. Accessed: Sep. 12, 2018. [Online]. Available: http://licensing.fcc.gov/myibfs/forwardtopublictabaction.do?f
[6] S. H. Blumenthal, "Medium Earth orbit Ka band satellite communications system," in *Proc. IEEE Mil. Commun. Conf.*, Nov. 2013, pp. 273–277.
[7] *LeoSat Non-Geostationary Satellite System Attachment A: Technical Annex to Supplement Schedule S*. Accessed: Mar. 20, 2018. [Online]. Available: http://licensing.fcc.gov/myibfs/download. do attachment key=115822
[8] M. A. Sturza, "The teledesic satellitesystem: Overview and design trades," in *Proc. Annu. Wireless Symp.*, Feb. 1995, pp. 402–409.
[9] D.P. Patterson, "Teledesic: A global broadband network," in *Proc. IEEE Aerosp. Conf. Proc.*, Mar. 1998, pp. 547–552.
[10] R. J. Leopold, "The Iridium communications systems," in *Proc. ICCS/ISITA*, Singapore, Nov. 1992, pp. 451–455.
[11] R. J. Leopold, "Low-Earth orbit global cellular communications network," in *Proc. Int. Conf. Commun. Conf. Rec.*, Jun. 1981, pp. 1108–1111.
[12] R. Wiedeman, A. Salmasi, and D. Rouffet, "Globalstar—Mobile communications where ever you are," in *Proc. 14th Int. Commun. Satellite Syst. Conf. Exhibit*, Sep. 1992, p. 1912.
[13] G. Comparetto and N. Hulkower, "Global mobile satellite communications - A review of three contenders," in *Proc. 15th Int. Commun. Satellite Syst. Conf. Exhibit*, 1994, p. 1138.
[14] J. V. Evans, "Satellite systems for personal communications," *IEEE Antennas Propag. Mag.*, vol. 39, no. 3, pp. 7–20, Jul. 1998.
[15] J. V. Evans, "Proposed U.S. Global satellite systems operating at Ka-Band," in *Proc. IEEE Aerosp. Conf. Proc.*, Vol. 4, Mar. 1998, pp. 525–537.
[16] G. B. Shaw, D. W. Miller, and D. E. Hastings, "The generalized information network analysis methodology for distributed satellite systems," Ph.D. dissertation, Dept. Aeronaut. Astronaut., Massachusetts Inst. Technol., Cambridge, MA, USA, 1999.
[17] I. del Portillo, B. G. Cameron, and E. F. Crawley, "A technical comparison of three low Earth orbit satellite constellation systems to provide global broadband," *Acta Astronautica*, vol. 159, pp. 123–135, Jun. 2019.
[18] *Propagation Data and Prediction Methods Required for the Design of Earth-Space Telecommunication Systems*, document Recommendation ITU-R618íC13, 2017.
[19] E. Altman and T. Jimenez, "NS simulator for beginners," *Synth. Lectures Commun. Netw.*, vol. 5, no. 1, p. 184. 2012.

SHIYI XIA (S'19) received the B.S. degree in communication and information engineer from Shanghai University, Shanghai, China, in 2017. He is currently pursuing the Ph.D. degree with the Innovation Academy for Microsatellites of CAS, Shanghai.

QUANJIANG JIANG was born in Cixi, Zhejiang, China. He received the B.S. and M.S. degrees in communication and information engineering from Xidian University, Xi'an, China, in 2007, and the Ph.D. degree in communication and information system from the University of Chinese Academy of Sciences, Beijing, China, in 2014.

He is currently the Director of the Communication Measurement and Control Technology Research Office, Institute of Electronic Information Technology, Institute of Microsatellite Innovation, Chinese Academy of Sciences.

He is mainly engaged in the research of low-orbit satellite wireless communication technology, especially in the field of low-orbit satellite Internet and the Internet of Things communication access technology. In recent years, he has published more than ten articles and more than ten patents.

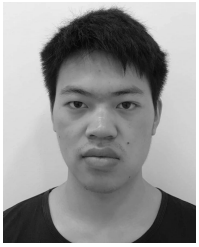

CHENG ZOU received the B.S. degree in communication engineering from Lanzhou University, Lanzhou, China, in 2017. He is currently pursuing the Ph.D. degree in communication and information system engineering with ShanghaiTech University.

GUOTONG LI received the B.S. degree in computer science and the master's degree in cryptography from the PLA Information Engineering University, in 1996, and the Ph.D. degree in communication and information systems from Zhejiang University, in 1999. He is currently an Associate Dean with the School of Aeronautics and Astronautics, University of Chinese Academy of Sciences.

In 2001, he was a Postdoctoral Fellow with the Shanghai Institute of Microsystems, Chinese Academy of Sciences. He has long been engaged in satellite communication systems, navigation system design, application basic research, and development work. From 1999 to 2003, he participated in the Innovation No. 1 Communication Small Satellite Project of the Chinese Academy of Sciences, responsible for the development of application systems.

From 2005 to 2009, he served as the Deputy General Manager of Shanghai Galileo Navigation Company and participated in the Galileo international cooperation project. Since 2009, he has been employed as an Expert in the overall national science and technology major expert group, and participated in the development of a new generation Beidou navigation systems. He is currently the Chief Commander of the satellite system. As the person in charge, he has undertaken more than ten projects of 863, Chinese Academy of Sciences and Shanghai. He has received many first prizes in Shanghai Science and Technology Progress Award, Second Prize in Military Science and Technology Progress, Outstanding Achievement Award of the Chinese Academy of Sciences, and CCTV 2015 Innovation Team Award. He has published more than 60 articles and applied for 19 patents.